IEEE Access
Multidisciplinary | Rapid Review | Open Access Journal

Received January 25, 2019, accepted February 20, 2019, date of publication February 26, 2019, date of current version March 29, 2019.

Digital Object Identifier 10.1109/ACCESS.2019.2901494

Effective Estimation of Integer Carrier Frequency Offset in LTE Downlink Systems With Symbol Timing Error

YONG-AN JUNG[1], MOO-YOUNG KIM[2], HYOUNG-KYU SONG[2], AND YOUNG-HWAN YOU[1]
[1]Department of Computer Engineering, Sejong University, Seoul 143-147, South Korea
[2]Department of Information and Communication Engineering, Sejong University, Seoul 143-147, South Korea

Corresponding author: Young-Hwan You (yhyou@sejong.ac.kr)

This work was supported in part by the Unmanned Vehicles Advanced Core Technology Research and Development Program through the National Research Foundation of Korea (NRF), in part by the Unmanned Vehicle Advanced Research Center (UVARC) funded by the Ministry of Science and ICT, South Korea, under Grant NRF-2017M1B3A2A01049997, and in part by the Ministry of Science and ICT (MSIT), South Korea, through the Information Technology Research Center (ITRC) Support Program supervised by the Institute for Information and Communications Technology Promotion (IITP) under Grant IITP-2018-2018-0-01423.

ABSTRACT An effective integer carrier frequency offset (IFO) detection scheme is proposed in the long-term evolution downlink system without relying on the knowledge of the cell ID (CID) that is carried through the synchronization signal. To enable IFO detection without relying on the CID, the proposed IFO detection method utilizes the symmetric property of the synchronization signal, such as the primary synchronization signal (PSS) and the secondary synchronization signal (SSS). This design avoids the need to retrieve the CID that is carried by the PSS and the SSS at the IFO-matching stage. In addition to investigating the usefulness of the proposed IFO detection method, the probability of detection failure is theoretically calculated. The simulation results demonstrate that both the synchronization signals are effectively exploited for the robust detection of the IFO in the presence of non-negligible symbol timing error, where the conventional approaches show unsatisfactory performance.

INDEX TERMS Long term evolution, carrier frequency offset, synchronization signal, symbol timing error.

I. INTRODUCTION

Orthogonal frequency division multiplexing (OFDM) has been commonly used in wireless broadband networks thanks to its high spectral efficiency and resilience against fading distortions. Due to its appealing benefits, OFDM has been considered as a modulation scheme for a number of commercial applications, including the digital video broadcasting-terrestrial (DVB-T), the IEEE 802.11n wireless local area network (WLAN), and the long term evolution (LTE) [1]–[3]. In LTE, orthogonal frequency division multiple access (OFDMA) is used in the downlink (DL) to enhance robustness to fading impairments at an enhanced base station (BS), whereas single-carrier frequency division multiple access (SC-FDMA) is adopted in the uplink (UL) to mitigate the effect of the peak-to-average power-ratio at the user equipment (UE). The LTE-PHY is a very effective way to carry both data and control signal between the BS and mobile UE.

In the LTE system, it is crucial for UE to connect a communication link with the best serving BS as soon as possible. For this purpose, the UE has not only to detect symbol timing offset (STO) and carrier frequency offset (CFO) but also to acquire the cell ID (CID) [5]–[18]. Due to the sensitivity of OFDM to time and frequency imperfections, there is a need for fast cell search procedure that synchronizes the UE and the BS so that the orthogonality of subcarriers can be maintained and the cell can be identified. An LTE cell is recognized by the CID message transmitted through the synchronization signals such as primary synchronization signal (PSS) and secondary synchronization signal (SSS) [8]–[18]. The LTE cell search procedure is in general classified into three steps. In the first step, the redundant guard interval (GI) is used to find the fractional CFO (FFO) and initial STO [6], [7]. Once this phase is finished, the sector ID (SID) and integer CFO (IFO) are jointly estimated using the PSS [8]–[15]. Finally, the frame

The associate editor coordinating the review of this manuscript and approving it for publication was Wenchi Cheng.

boundary and the group ID (GID) are determined using the SSS [16]–[18], thus resolving the radio timing for the DL transmission. Since the receiver can perform SSS detection only after the PSS is successfully recognized, PSS detection is an important part of the overall cell search procedure. In [7] and [8], PSS detection scheme was presented to be accomplished in the time domain (TD). The presence of IFO deteriorates the detection accuracy of the PSS in the TD. To address this problem, synchronization and cell search have been presented by identifying the PSS in the frequency domain (FD) [9]–[15], wherein the IFO is jointly estimated along with the SID. The IFO detection is typically accomplished in a joint or sequential manner. In [9]–[13], IFO detection can be jointly performed during the PSS-matching process, which is performed evaluating the cross-correlation for phase difference of the received PSS and the original PSS. Therefore, the IFO and SID can be jointly detected using the correlator banks for a large number of hypotheses, which demands a massive amount of processing loads. To ease the computational burden, a sequential IFO and SID detection has been proposed using differential correlation [14], [15]. In this approach, the central-symmetry property of the PSS is used to detect the IFO without any information of the SID. Therefore, this strategy can decouple the joint search space of a number of hypotheses into two reduced search spaces. However, this approach is sensitive to the presence of residual STO, thereby reducing its ability to detect the IFO. It is therefore necessary to develop low-cost and robust synchronization algorithm for the UE's simple operation in the LTE system.

In this paper, an effective IFO detection method is proposed in the LTE DL system. The symmetry property present in two synchronization signals facilitates detection of IFO without a priori knowledge on the CID information. To examine the usefulness of the proposed IFO detection scheme, the probability of failure of the proposed IFO detection scheme is analytically derived. Simulation results show that the proposed IFO detection scheme provides robustness against the presence of residual STO with reduced complexity, compared with the existing IFO detection method.

The rest of this paper is organized as follows. Next section introduces a signal model adopted in this paper. The existing IFO detection methods based on differential correlation are presented in Section III. Section IV proposes an efficient IFO estimation scheme independent of the transmitted PSS and SSS in the LTE DL. Section V presents experimental results to verify the effectiveness of the proposed IFO detection scheme. Section VI draws the conclusion of this paper.

II. SYSTEM DESCRIPTION

A. SIGNAL MODEL

We consider an OFDM system that consists of N non-zero subcarriers and N_g guard interval (GI) samples. After performing an N-point inverse FFT (IFFT) on the information symbols and adding GI at the front of the OFDM symbol to mitigate the detrimental effect of inter-symbol interference (ISI), an OFDM symbol with the duration of $N_u T_s$ is generated, where T_s is the sampling period and $N_u = N + N_g$. Since the FFO does not affect the performance of the IFO detector like the existing approaches [12]–[15], we assume the perfect recovery of FFO. The existence of multipath fading may greatly deteriorate the accuracy of the STO estimate. For this reason, it is assumed that the residual STO remains after initial timing estimation process. Bearing these assumptions in mind, the TD signal during the l-th period $y_l(m)$, $m = -N_g, -N_g+1, \cdots, N-1$, appears as [11]

$$y_l(m) = e^{jl\nu\rho} e^{j2\pi\nu(m-\tau)/N} h_l(m) \otimes x_l(m-\tau) + z_l(m) \quad (1)$$

where $\rho = 2\pi N_g/N$, ν denotes the IFO, τ denotes the STO, $x_l(m)$ is the m-th sample over the l-th symbol duration, $h_l(m)$ is the impulse response of the channel, $\otimes$ is the linear convolution, and $z_l(m)$ is the contribution of the thermal noise that is modeled as a zero-mean additive white Gaussian noise (AWGN). Removing the GI and taking the FFT, the FD signal in the k-th subcarrier during the l-th symbol can be written as [12]

$$Y_l(k) = H_l(k-\nu) X_l(k-\nu) e^{-j2\pi(k-\nu)\tau/N} e^{jl\nu\rho} + Z_l(k) \quad (2)$$

where $X_l(k)$ is the symbol transmitted at the k-th subcarrier, $H_l(k)$ denotes the frequency response of the channel, and $Z_l(k)$ represents a complex zero-mean AWGN with variance σ_Z^2.

B. SYNCHRONIZATION SIGNAL

The position of the PSS and SSS in the LTE frame depends on the duplex mode used to separate UL and DL traffic. We consider the LTE DL system operating with frequency division duplex (FDD) mode. As shown in Fig. 1, the radio frame in LTE is 10ms long, which is divided into ten 1ms long subframe. Each subframe is made up of two 0.5ms long slots. Every slot is divided into 7 OFDM symbols in the case of a normal CP, while 6 OFDM symbols are included in each slot for an extended CP. In LTE DL, the PSS and SSS structure is specifically designed to facilitate the acquisition of cell information. For this purpose, three polyphase Zadoff-Chu (ZC) sequences with sequence index u are adopted in the PSS. The PSS sequence is mapped onto the 72 central subcarriers across DC, which consists of 62 plus 10 guard subcarriers. They are defined as [3]

$$P_u(k) = \begin{cases} e^{-j\pi u(k+31)(k+32)/63}, & k \in \mathcal{S} \\ 0, & \text{otherwise}, \end{cases} \quad (3)$$

where $\mathcal{S} = \{k \,||k| \le N_p/2, k \ne 0\}$, the ZC root sequence index $u \in \{25, 29, 34\}$ depending on SIDs, and N_p denotes the number of non-zero PSS subcarriers.

The main purpose of the SSS is to recognize the GID and to find the starting position of an LTE frame. The SSS sequence forms binary phase-shift keying (BPSK) signal, which is derived from two length-31 scrambled and cyclically shifted binary sequences $s_0^{(w_0)}(n)$ and $s_1^{(w_1)}(n)$, with

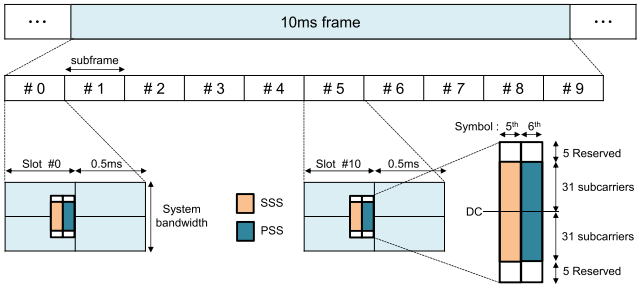

FIGURE 1. Synchronization signal and slot structure in the LTE FDD case.

$n = 0, 1, \cdots, N_p/2 - 1$. Thus, a FD sequence $C(n)$, $0 \leq n < N_p$, are defined as

$$C(2n) = \begin{cases} s_0^{(w_0)}(n)c_0(n) & \text{in subframe 0} \\ s_1^{(w_1)}(n)c_0(n) & \text{in subframe 5} \end{cases} \tag{4}$$

$$C(2n+1) = \begin{cases} s_1^{(w_1)}(n)c_1(n)d_1^{(w_0)}(n) & \text{in subframe 0} \\ s_0^{(w_0)}(n)c_1(n)d_1^{(w_1)}(n) & \text{in subframe 5} \end{cases} \tag{5}$$

where $c_i(n)$ and $d_1^{(w_i)}(n)$ denote the scrambling sequences to randomize the interference between different cells. The indices w_0 and w_1 are present to univocally decide the GID. The sequence $C(n)$ is mapped onto $S(k)$ with subcarrier indices $k \in \mathcal{S}$. In FDD mode, the PSS is present in the last two OFDM symbol of slots 0 and 10 in a frame, whereas the SSS is located in the second last two OFDM symbol of slots 0 and 10. For notational convenience, we use $X_l(k)$ to denote the PSS and SSS defined by

$$X_{l+v}(k) = \begin{cases} S(k), & v = 0 \\ P_u(k), & v = 1. \end{cases} \tag{6}$$

Typically, a two-stage CID detection strategy has been considered to enhance the cell search performance in the LTE system [16]–[18]. In this case, the CID is obtained by combining the IDs on PSS and SSS. The first stage is to decide the SID by finding the PSS and the SSS is detected to extract the GID during the successive stage. As can be seen in (2) and (6), the unknown parameters v and u jointly contribute to the received signal $Y_l(k)$, thereby necessitating the use of joint estimation in the conventional cell search schemes. The computational burden of the IFO detection is significantly decreased if it is accomplished together with PSS detection since there are only three PSS sequences compared to 168 SSS sequences.

III. CONVENTIONAL DETECTION METHOD

The IFO detection is usually performed in the FD [12]–[15] in a coherent or non-coherent manner. The coherent detection strategy requires a priori knowledge on the channel state information (CSI). However, the CSI has not been known during the cell search stage. To solve this problem, non-coherent detection in the FD has been proposed using differential correlation. For this reason, this paper focuses on non-coherent detection method. Assuming that $H_l(k) \approx H_l(k-1)$, the differential correlation from neighboring subcarriers of the received PSS signal can be used to mitigate the impact of the channel fading and STO on the estimation accuracy

$$\begin{aligned} \bar{Y}_{l+1}(k) &= Y_{l+1}(k)Y_{l+1}^*(k-1) \\ &\approx |H_{l+1}(k-v)|^2 D_u(k-v)e^{j2\pi\tau/N} \\ &\quad + \bar{Z}_{l+1}(k), \quad k \in [-30,-1] \cup [2,31] \end{aligned} \tag{7}$$

where $(\cdot)^*$ denotes the complex conjugate operation, $D_u(k) = P_u(k)P_u^*(k-1)$ is the differential relation between two neighboring PSS subcarriers, and $\bar{Z}_{l+1}(k)$ is a complex zero-mean combined noise contribution.

A. ALMOST HALF COMPLEXITY DETECTION (AHCD) SCHEME

A reduced complexity IFO detection method is presented using inherent central-symmetric property of the ZC sequences [8]. In this approach, the IFO can be estimated performing the FD shift of the PSS at the receiver. The objective function $\Omega_p(u, i)$ of the joint detection scheme is given by

$$\Omega_a(u,i) = \sum_{k=2}^{N_p/2} \left\{ \bar{Y}_{l+1}(k+i) + \bar{Y}_{l+1}^*(-k+i+1) \right\} D_u^*(k) \tag{8}$$

where i is the hypothesized IFO. By finding the peak of the metric $\Omega_a(u, i)$ with respect to u and i, the joint estimate of the IFO and SID is constructed by

$$(\hat{u}, \hat{v}) = \underset{|i| \leq M, u \in \{25,29,34\}}{\arg\max} |\Omega_a(u,i)| \tag{9}$$

where M is the finite number of possibilities of v. To estimate the IFO and SID concurrently, this kind of detection strategy requires the correlation banks for $3(2M+1)$ hypotheses. Although a half-length complex correlation between the received ZC sequence and the original sequence reduces a computational complexity, it still demands a significant processing load. Another drawback of this scheme is that the peaks of the differential correlation are very similar for different IFO hypotheses, deteriorating the detection accuracy of the IFO.

B. SEQUENTIAL IFO AND SID DETECTION (SISID) SCHEME

To detect the IFO regardless of the SID, a low-complexity IFO detection scheme without the PSS-matching process is proposed in [14]. Since the local differential reference with the SID u is conjugate symmetric with respect to the origin so that $D_u(k) = D_u^*(-k+1)$, the objective function can be designed to be

$$\Omega_b(i) = \sum_{k=2}^{N_p/2} \bar{Y}_{l+1}(k+i)\bar{Y}_{l+1}(-k+i+1) \tag{10}$$

which facilitates the joint detection task to be decoupled into a series of single parameter estimation problems. Consequently, the IFO estimation is carried out first, followed by

the SID detection as follows

$$\hat{\nu} = \arg\max_{|i|\le M} \Re\{\Omega_b(i)\} \tag{11}$$

and

$$\hat{u} = \arg\max_{u\in\{25,29,34\}} \Re\{\Omega_a(u,\hat{\nu})\} \tag{12}$$

where $\Re\{\cdot\}$ denotes the real component of the enclosed quantity. A drawback of this scheme is that the effect of residual STO turns out to be doubled compared to (9).

C. NORMALIZED SEQUENTIAL IFO AND SID DETECTION (NSISID) SCHEME

In [15], a sequential IFO and SID detection scheme is proposed using the symmetric characteristic of the PSS. This approach uses a normalized received PSS to remove the effect of the magnitude of the channel, which produces the channel-compensated objective function

$$\Omega_c(i) = \frac{1}{N_p/2-1}\sum_{k=2}^{N_p/2} \tilde{Y}_{l+1}(k+i)\tilde{Y}_{l+1}(-k+i+1) \tag{13}$$

where $\tilde{Y}_{l+1}(k) = \bar{Y}_{l+1}(k)/|\bar{Y}_{l+1}(k)|$. By looking for the minimum of the objective function $|\Omega_c(i)-1|$, the IFO is estimated by

$$\hat{\nu} = \arg\min_{|i|\le M} |\Omega_c(i)-1|\,. \tag{14}$$

Since such a design decouples the estimation of the IFO and SID, the SID is sequentially retrieved as follows

$$\hat{u} = \arg\max_{u\in\{25,29,34\}} \Re\{\Omega_d(u,\hat{\nu})\} \tag{15}$$

where $\Omega_d(u,\hat{\nu}) = \sum_{k=2}^{N_p/2}\{\tilde{Y}_{l+1}(k+\hat{\nu}) + \tilde{Y}^*_{l+1}(-k+\hat{\nu}+1)\}D^*_u(k)$. Since it is most important to design the synchronization receiver with a low power consumption, compromises between the detection performance and computational burden have to be done carefully.

IV. PROPOSED DETECTION METHOD

This section presents an effective IFO detection scheme using inherent symmetric characteristics of the synchronization signals in the LTE system. The symmetric property can be integrated for IFO detection without relying on the CID. To examine the effectiveness of the proposed IFO detection method, the probability of failure of the IFO estimator is theoretically derived.

A. ESTIMATION ALGORITHM

Based on the assumption $H_l(k) \approx H_{l+1}(k)$, we compute temporal correlation between the received PSS and SSS in the FD to remove the effect of channel fading as follows

$$\begin{aligned} R_l(k) &= Y^*_l(k)Y_{l+1}(k) \\ &\approx |H_l(k-\nu)|^2 S^*(k-\nu)P_u(k-\nu)e^{j\nu\rho} + W_l(k) \end{aligned} \tag{16}$$

where

$$\begin{aligned} W_l(k) &= H^*_l(k-\nu)S^*(k-\nu)Z_{l+1}(k)e^{j2\pi(k-\nu)\tau/N}e^{-jl\nu\rho} \\ &\quad + H_{l+1}(k-\nu)P_u(k-\nu)Z^*_l(k)e^{-j2\pi(k-\nu)\tau/N}e^{j(l+1)\nu\rho} \\ &\quad + Z^*_l(k)Z_{l+1}(k). \end{aligned} \tag{17}$$

In (17), $W_l(k)$ has a zero mean and variance of σ^2_W. Then, the symmetry property of the PSS and SSS is utilized to enable the estimation of the IFO without any information of the CIDs. First, to perform the IFO detection without knowledge of the transmitted PSS, we use conjugate-symmetric correlation

$$\begin{aligned} \bar{R}_l(k) &= R_l(k)R^*_l(-k) \\ &= |H_l(k-\nu)|^2|H_l(-k-\nu)|^2\bar{S}(k-\nu)\bar{P}_u(k-\nu) \\ &\quad + \bar{W}_l(k), \quad 1\le k\le N_p/2 \end{aligned} \tag{18}$$

where $\bar{S}(k) = S^*(k)S(-k)$, $\bar{P}_u(k) = P_u(k)P^*_u(-k)$, and $\bar{W}_l(k)$ is the combined AWGN given by

$$\begin{aligned} \bar{W}_l(k) &= |H_l(k-\nu)|^2 S^*(k-\nu)P_u(k-\nu)W^*_l(-k)e^{j\nu\rho} \\ &\quad + |H_l(-k-\nu)|^2 S(-k-\nu)P^*_u(-k-\nu)W_l(k)e^{-j\nu\rho} \\ &\quad + W_l(k)W^*_l(-k). \end{aligned} \tag{19}$$

Since the PSS has symmetrical pattern in the FD and the SSS has a TD conjugate symmetry, it is obvious that $\bar{S}(k) = \pm E_X$ and $\bar{P}_u(k) = E_X$ when no IFO is present, where $E_X = |S(k)|^2 = |P_u(k)|^2$ represents the symbol energy of the synchronization signal. With these properties in mind, the objective function $\Omega_p(i)$ of IFO detection is defined as

$$\Omega_p(i) = \sum_{k=1}^{N_p/2} \bar{R}^2_l(k+i) \tag{20}$$

which eliminates the need to rely on the transmitted SSS. Putting (18) to (20) leads to

$$\begin{aligned} \Omega_p(i) &= \sum_{k=1}^{N_p/2} |H_l(k+i-\nu)|^4|H_l(-k+i-\nu)|^4 \\ &\quad \times \bar{S}^2(k+i-\nu)\bar{P}^2_u(k+i-\nu) + \sum_{k=1}^{N_p/2}\tilde{W}_l(k+i) \end{aligned} \tag{21}$$

where

$$\begin{aligned} \tilde{W}_l(k) &= 2|H_l(k-\nu)|^2|H_l(-k-\nu)|^2\bar{S}(k-\nu) \\ &\quad \times \bar{P}_u(k-\nu)\bar{W}_l(k) + \bar{W}^2_l(k). \end{aligned} \tag{22}$$

Since $\bar{S}(k+i-\nu) = \pm E_X$ and $\bar{P}_u(k+i-\nu) = E_X$ regardless of u when $i=\nu$, (21) can be simplified to

$$\begin{aligned} \Omega_p(i) &= E^4_X \sum_{k=1}^{N_p/2} |H_l(k+i-\nu)|^4|H_l(-k+i-\nu)|^4 \\ &\quad + \sum_{k=1}^{N_p/2}\tilde{W}_l(k+i) \end{aligned} \tag{23}$$

which indicates that the value of $\Omega_p(i)$ is independent of the PSS and SSS. If $i \ne \nu$, it can be seen that $\bar{S}^2(k+i-\nu)$ is still equal to E^2_X, whereas $\bar{P}^2(k+i-\nu)$ is either zero or

unknown random sequence depending on the amount of ν. In this hypothesis, we have

$$\Omega_p(i) = E_X^2 \sum_{k=1}^{N_p/2} |H_l(k+i-\nu)|^4 |H_l(-k+i-\nu)|^4 \times \bar{P}_u^2(k+i-\nu) + \sum_{k=1}^{N_p/2} \tilde{W}_l(k+i). \quad (24)$$

As a result, the criterion for IFO detection can be formulated as

$$\hat{\nu} = \arg\max_{|i|\le M} \Re\{\Omega_p(i)\}. \quad (25)$$

To identify the PSS, the SID detection can be performed using (12).

B. PROBABILITY OF DETECTION FAILURE

Let $P_f = \text{Prob}\{\hat{\nu} \neq \nu\}$ denote the probability of failure of the IFO estimator. In the AWGN channel, we derive the probability of failure of (25). Under the hypothesis that $i = \nu$, the real part of (23) follows Gaussian distribution with mean $\mu = N_p E_X^4/2$ and variance $\sigma_1^2 = N_p(E_X^4\sigma_{\tilde{W}}^2 + 3\sigma_{\tilde{W}}^4/4)$, where $\sigma_{\tilde{W}}^2$ is the variance of (19) given by

$$\begin{aligned}\sigma_{\tilde{W}}^2 &= 2E_X^2\sigma_W^2 + \sigma_W^4 \\ &= 2E_X^2(2E_X\sigma_Z^2 + \sigma_Z^4) + (2E_X\sigma_Z^2 + \sigma_Z^4)^2. \end{aligned} \quad (26)$$

When $i \neq \nu$, on the other hand, the probability density function of $\Re\{\Omega_p(i)\}$ is treated as a zero-mean Gaussian random variable (RV) with variance $\sigma_0^2 = N_p(E_X^4\sigma_{\tilde{W}}^2 + 3\sigma_{\tilde{W}}^4/4)$. Let $z = \Re\{\Omega_p(i)\}$. If IFO occurs equally likely within the range of $|\nu| \le M$, the probability of failure is defined as

$$P_f = 1 - \int_{-\infty}^{\infty} \frac{1}{\sqrt{2\pi\sigma_1^2}} e^{-\frac{(z-\mu)^2}{2\sigma_1^2}} \left[1 - Q\left(\frac{z}{\sigma_0}\right)\right]^{2M} dz \quad (27)$$

where $Q(z)$ denotes the Q-function given by

$$Q(z) = \frac{1}{\sqrt{2\pi}} \int_z^{\infty} e^{-\frac{x^2}{2}} dx. \quad (28)$$

To proceed further, we use a tight upper bound of $Q(z)$ given by [19]

$$\begin{aligned} Q\left(\frac{z}{\sigma_0}\right) &\le \frac{1}{\pi} \int_{\theta_{i-1}}^{\theta_i} e^{-\frac{z^2}{2(\sin^2\theta_i)\sigma_0^2}} d\theta \\ &= \sum_{i=1}^{N_e} a_i e^{-\frac{b_i z^2}{2\sigma_0^2}} \end{aligned} \quad (29)$$

where $a_i = (\theta_i - \theta_{i-1})/\pi$ and $b_i = 1/\sin^2\theta_i$ with $0 = \theta_0 \le \theta_1 \cdots \le \theta_{N_e} = \pi/2$. Note that the bound tends to the exact value by increasing N_e. Thus, the upper bound of (27) is obtained as

$$P_f \le 1 - \int_{-\infty}^{\infty} \frac{1}{\sqrt{2\pi\sigma_1^2}} e^{-(z-\mu)^2/2\sigma_1^2} \times \left[1 - \sum_{i=1}^{N_e} a_i e^{-\frac{b_i z^2}{2\sigma_0^2}}\right]^{2M} dz. \quad (30)$$

Using multinomial theorem, it immediately follows that

$$P_f \le 1 - \sum_{\nu_1+\cdots+\nu_{N_e+1}=2M} \prod_{i=1}^{N_e} (-a_i)^{\nu_i} \binom{2M}{\nu_1, \nu_2, \cdots, \nu_{N_e+1}} \times \underbrace{\frac{1}{\sqrt{2\pi\sigma_1^2}} \int_{-\infty}^{\infty} e^{-\frac{(z-\mu)^2}{2\sigma_1^2}} e^{-\frac{z^2}{2\sigma_0^2}\sum_{i=1}^{N_e} b_i\nu_i} dz}_{P_\nu} \quad (31)$$

where a multinomial coefficient takes form

$$\begin{aligned}\binom{2M}{\nu_1, \nu_2, \cdots, \nu_{N_e+1}} &= \binom{\nu_1}{\nu_1}\binom{\nu_1+\nu_2}{\nu_2} \\ &\cdots \binom{\nu_1+\nu_2+\cdots+\nu_{N_e+1}}{\nu_{N_e+1}}. \end{aligned} \quad (32)$$

After some manipulations, P_ν can be expressed in a closed form

$$P_\nu = \left(1 + \frac{\sigma_1^2}{\sigma_0^2}\sum_{i=1}^{N_e} b_i\nu_i\right)^{-1/2} e^{-\frac{\mu^2}{2\sigma_1^2}\left\{1 - \left(1+\frac{\sigma_1^2}{\sigma_0^2}\sum_{i=1}^{N_e} b_i\nu_i\right)^{-1}\right\}}. \quad (33)$$

Substituting (33) to (31) yields

$$P_f \le 1 - \sum_{\nu_1+\cdots+\nu_{N_e+1}=2M} \prod_{i=1}^{N_e} (-a_i)^{\nu_i} \binom{2M}{\nu_1, \nu_2, \cdots, \nu_{N_e+1}} \times \left(1 + \frac{\sigma_1^2}{\sigma_0^2}\sum_{i=1}^{N_e} b_i\nu_i\right)^{-1/2} e^{-\frac{\mu^2}{2\sigma_1^2}\left\{1 - \left(1+\frac{\sigma_1^2}{\sigma_0^2}\sum_{i=1}^{N_e} b_i\nu_i\right)^{-1}\right\}}. \quad (34)$$

From μ^2, σ_0^2, and σ_1^2, it follows that $\sigma_1^2 = \sigma_0^2$ and

$$\frac{\mu^2}{\sigma_1^2} = \frac{N_p}{4(2\bar{\gamma} + \bar{\gamma}^2) + 3(2\bar{\gamma} + \bar{\gamma}^2)^2} \quad (35)$$

with

$$\bar{\gamma} = \frac{1}{\gamma}\left(2 + \frac{1}{\gamma}\right) \quad (36)$$

where $\gamma = E_X/\sigma_Z^2$ is the signal-to-noise ratio (SNR). Eventually, the upper bound of the probability of failure of (25) is obtained with respect to (35)

$$P_f \le 1 - \sum_{\nu_1+\cdots+\nu_{N_e+1}=2M} \prod_{i=1}^{N_e} (-a_i)^{\nu_i} \times \binom{2M}{\nu_1, \nu_2, \cdots, \nu_{N_e+1}} \left(1 + \sum_{i=1}^{N_e} b_i\nu_i\right)^{-1/2} \times e^{-\frac{N_p}{8(2\bar{\gamma}+\bar{\gamma}^2)+6(2\bar{\gamma}+\bar{\gamma}^2)^2}\left\{1 - \left(1+\sum_{i=1}^{N_e} b_i\nu_i\right)^{-1}\right\}}. \quad (37)$$

V. SIMULATION RESULTS

The accuracy of the presented detection methods is assessed in the LTE system with 15kHz subcarrier spacing and 5MHz bandwidth. In our simulations, the carrier frequency of 2GHz, the sampling time of $T_s = 0.1302\mu s$, the FFT size of $N = 512$, the GI length of $N_g = 128$, and QPSK modulation are considered. We adopt the Extended Pedestrian A (EPA), Extended Vehicular A (EVA), Extended Typical Urban (ETU), and Extended Delay Spread (EDS) channel models [21]. The main channel parameters are shown in Table 1. The channel taps are modeled as samples of statistically independent complex Gaussian RVs. Three Doppler frequencies are used to represent low, medium, and high speeds of 5Hz, 70Hz, and 300Hz, respectively. At the carrier frequency of 2GHz, these frequencies correspond to UE velocities of 2.7km/h, 37.8km/h, and 162km/h. From [12], the range for hypothesized IFO is $\{0, \pm1, \pm2, \pm3\}$, which amounts to putting $M = 3$. We assume that there is a random STO uniformly generated between 0 and τ_{max} samples, where τ_{max} denotes maximum STO.

TABLE 1. Channel parameters.

Model	No. of Channel taps	Maximum excess delay (μs)	Doppler frequency (Hz)
EPA	7	0.41	5
EVA	9	2.51	70
ETU	9	5.00	300
EDS	18	28.58	5

A. COMPUTATIONAL COMPLEXITY

The arithmetic complexity of the joint detection methods are discussed in the section. Table 2 lists the number of arithmetic operations of the detection methods required to calculate the corresponding objective functions, where $K = 2M + 1$. To fairly compare the processing load of the detection methods, the arithmetic operations in Table 2 are transformed to the number of real floating point operations (flops). For this purpose, we assume that one complex multiplication, one complex addition, one complex magnitude, and one complex square operations are equal to six, two, three, and four real flops, respectively [20]. The AHCD scheme requires $3N_p/2 - 3$ complex multiplications and $N_p - 3$ complex additions to calculate (8), which corresponds to $11N_p - 24$ flops. Therefore, the overall number of flops needed to get (9) is $3K(11N_p - 21)$. The SISID scheme demands $3N_p/2 - 3$ complex multiplications and $N_p/2 - 2$ complex additions to compute (10), which is equivalent to $10N_p - 22$ flops. Thus, the number of total flops used in (11) is $K(10N_p - 22)$. Since some operations are already available from (10), only $3(5N_p - 9)$ flops are needed to sequentially compute (12). In the case of the NSISID scheme, $15N_p - 28$ flops are required to get the quantity $|\Omega_c(m) - 1|$ so that (14) requires $K(15N_p - 28)$ flops. For the SID detection, $3(5N_p - 9)$ flops are required in (15). The proposed scheme computes (20) with $3N_p/2$ complex multiplications, $N_p/2 - 1$ complex additions, and $N_p/2$ complex squares, which are converted to $12N_p - 2$ flops. Considering the number of IFO trial values, $K(12N_p - 2)$ flops are needed in (25). In (12), $3(11N_p - 21)$ flops are further needed for the SID detection.

B. DETECTION PERFORMANCE

Fig. 2 shows the probability of failure of the IFO estimator, denoted by $P_f = \text{Prob}\{\hat{\nu} \neq \nu\}$, in the AWGN channel for various values of τ_{max}. To calculate (37), we choose $N_e = 2$ so that $a_1 = 1/16$, $a_2 = 1/4$, $b_1 = 1$, and $b_2 = 4/3$ [19]. From the presented results, it is observed that the simulated curve is in accordance with the upper bound calculated using (37). As expected, the approximation (29) leads to a very tight result and the upper bound is more accurate as the SNR increases. Furthermore, the probability of failure of the existing IFO estimation schemes is severely deteriorated with the increase in τ_{max}, whereas the performance of the proposed IFO detection scheme is constant to τ_{max}. The price for such a benefit is a certain degradation of detection performance in low SNR region, which is attributed by the SNR loss incurred from squaring the conjugate-symmetric correlation in (20). Because of its high sensitivity to residual STO, there are limitations to apply the existing methods to the LTE system especially for high SNR conditions.

Fig. 3 depicts the probability of failure of the IFO detection methods as a function of SNR in the EPA and EVA channels. Here, the timing error is fixed to $\tau_{max} = 10$ and $\tau_{max} = 20$ [10]. It can be seen that the increased frequency selectivity greatly affects the detection performance of the IFO estimation schemes. Apparently, this phenomenon is more prominent in the case of the conventional detection methods. The reason for this is that the conventional estimation schemes are based on the differential correlation between the neighboring subcarriers to eliminate the effect of channel fading.

To show the effect of time and frequency selectivity on the performance of the IFO detection schemes, the ETU channel with maximum Doppler frequency of 300Hz and the EDS channel with maximum excess delay of $25.58\mu s$ are considered in Fig. 4. The simulation parameters are the same as those in Fig. 3. It can be seen that the trend of the probability curves is qualitatively similar to that in Fig. 3. Since the conventional schemes are based on the differential correlation under the assumption $H_l(k) \approx H_l(k-1)$, its performance is severely degraded in a frequency selective fading channel wherein each subcarrier undergoes a different channel fading. Hence, the proposed scheme is more suitable for the IFO detection when STO is present in the frequency selective fading channel than the conventional schemes.

Fig. 5 shows the overall probability of failure of the joint detector, denoted by $P_o = \text{Prob}\{(\hat{u}, \hat{\nu}) \neq (u, \nu)\}$, using the same simulation scenarios to Figs. 3 and 4. Although the proposed approach adopts the existing SID detection scheme (12), which is sensitive to residual STO, the robustness of the proposed scheme to residual STO is still observed when compared to the benchmark methods. The observation

TABLE 2. Arithmetic operations of the detection methods.

Method	Operation	Complex multiplication	Complex addition	Complex magnitude	Complex square	Real multiplication
AHCD	(9)	$3K(3N_p/2-3)$	$3K(N_p-3)$	$3K$	-	-
SISID	(11)	$K(3N_p/2-3)$	$K(N_p/2-2)$	-	-	-
	(12)	$3(N_p/2-1)$	$3(N_p-3)$	-	-	-
NSISID	(14)	$K(3N_p/2-3)$	$K(N_p/2-2)$	$K(N_p-1)$	-	$K(2N_p-3)$
	(15)	$3(N_p/2-1)$	$3(N_p-3)$	-	-	-
Proposed	(25)	$3KN_p/2$	$K(N_p/2-1)$	-	$KN_p/2$	-
	(12)	$3(3N_p/2-3)$	$3(N_p-3)$	-	-	-

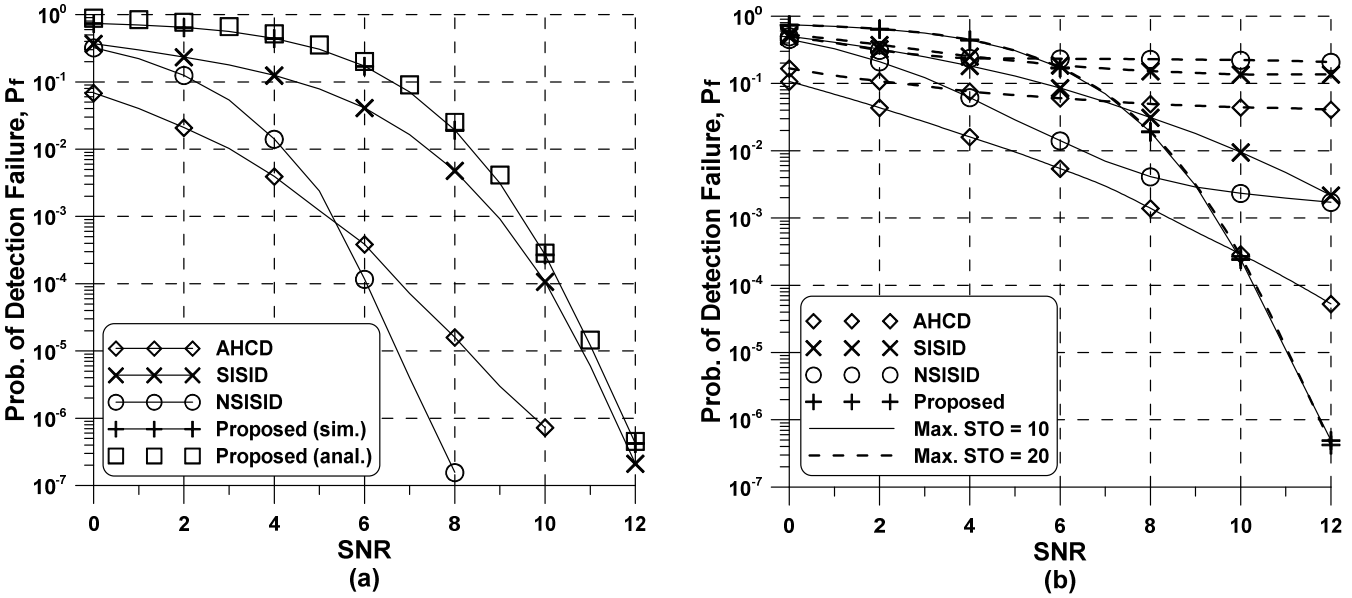

FIGURE 2. Performance of the IFO detectors in the AWGN channel: (a) $\tau_{max} = 0$ and (b) $\tau_{max} = 10$ and $\tau_{max} = 20$.

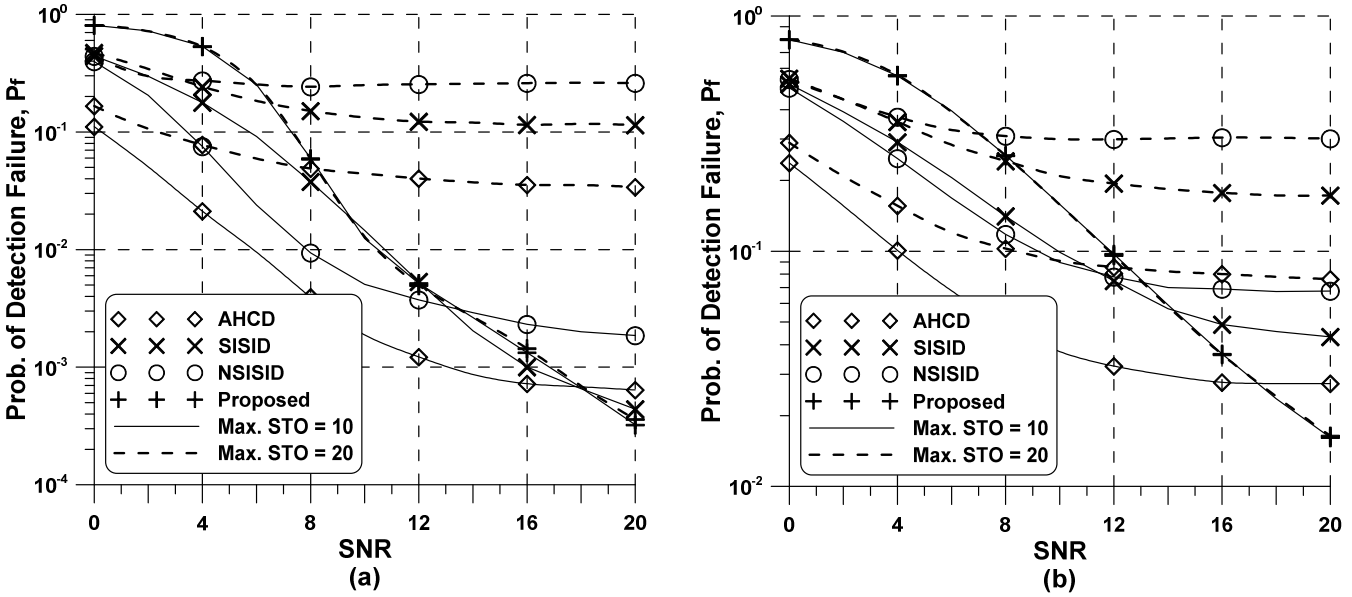

FIGURE 3. Performance of the IFO detectors with respect to SNR. (a) EPA channel. (b) EVA channel.

means that the overall performance of the synchronization receiver is mainly dominated by the performance of the IFO detector as discussed in [12]. Such a phenomenon can be explained by recognizing that the use of differential correlation in the conventional scheme and conjugate-symmetric correlation in the proposed scheme leads to similar peaks for

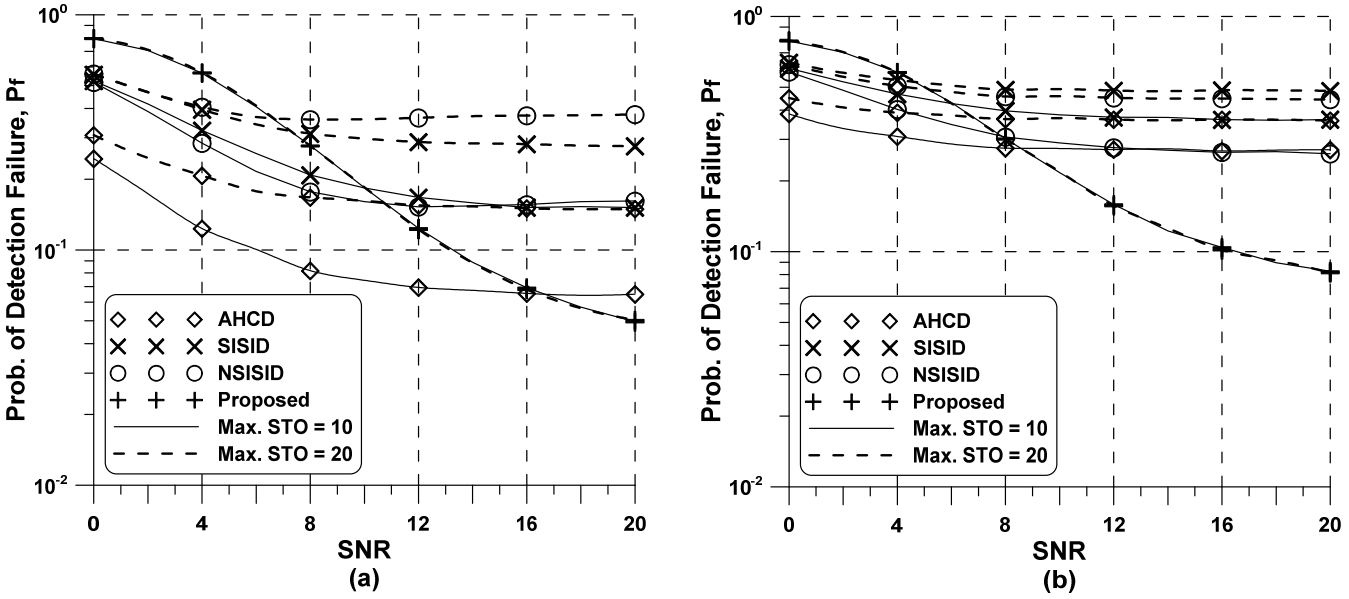

FIGURE 4. Performance of the IFO detectors with respect to SNR. (a) ETU channel. (b) EDS channel.

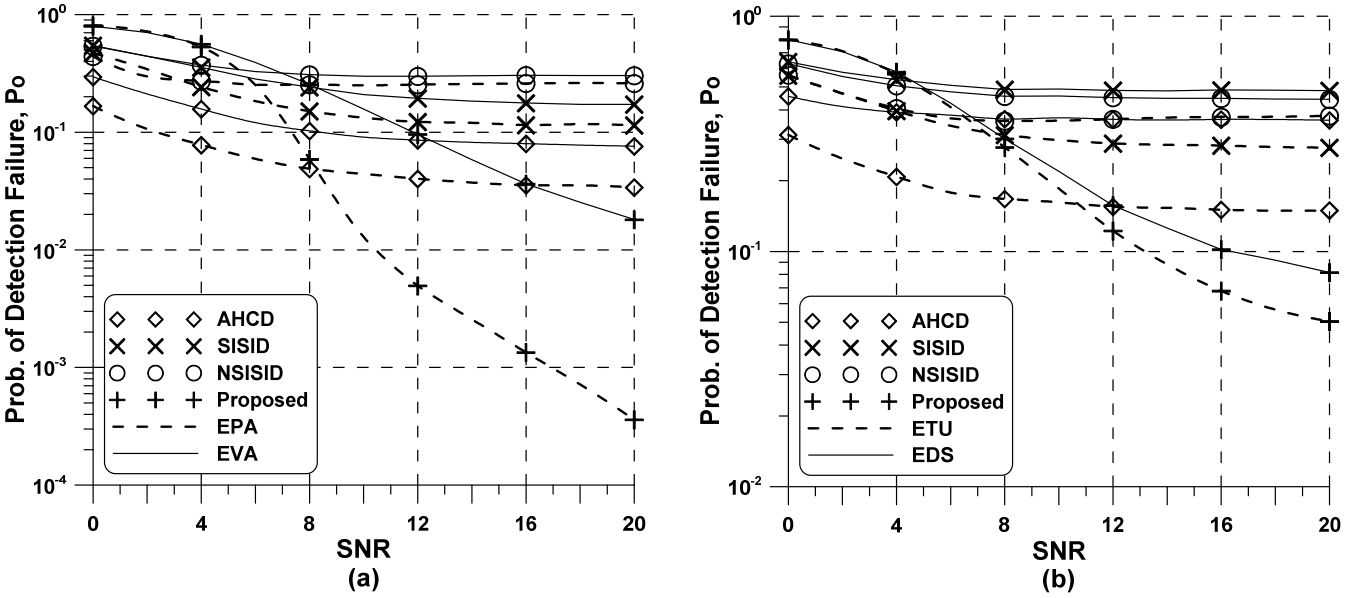

FIGURE 5. Overall performance of the joint detectors when $\tau_{max} = 20$. (a) EPA/EVA channel. (b) ETU/EDS channel.

different IFO hypotheses due to substantial loss of autocorrelation property of the original PSS, while the SID detection is still based on a good cross-correlation property between differential PSS sequences. Regarding the number of flops, the processing load of the proposed joint detection method is reduced by half relative to that of the AHCD scheme, whereas it has almost the same complexity to the NSISID scheme.

VI. CONCLUSION

To ensure a reliable cell search in LTE, it is crucial to perform IFO estimation without having to rely on the CID information. To address the problem, an effective IFO estimation method using inherent symmetric property of the synchronization signals is presented in the LTE DL system. The proposed IFO estimation scheme operates without relying on the knowledge of CID and exploits the correlation between the received PSS and SSS, which mitigates the impact of residual STO on the detection performance at the expense of a slight performance loss in low SNR region. To complete cell search, the conventional SID detection scheme is sequentially integrated with the proposed IFO detection scheme, and this strategy still provides improved performance in terms of overall detection probability due to its excellent ability to detect the IFO. It was demonstrated from simulation results that the

proposed detection scheme achieves acceptable performance in a harsh multipath channel having long delay spreads and non-negligible STO, compared with the existing detection methods.

REFERENCES

[1] *Digital Video Broadcasting (DVB); Frame Structure Channel Coding and modulation for a Second Generation Digital Terrestrial Television Broadcasting System (DVB-T2)*, Standard ETSI EN 302 755, Jul. 2015.

[2] *IEEE 802.11n standard. Part 11: Wireless LAN Medium Access Control (MAC) and Physical Layer (PHY) Specifications Amendment 5: Enhancements for Higher Throughput*, IEEE Standard 802.11n-2009, Oct. 2009.

[3] *LTE; Evolved Universal Terrestrial Radio Access (EUTRA); Physical Channels and Modulation (Release 10)*, document 3GPP TS 36.211, Jan. 2011.

[4] *LTE; Evolved Universal Terrestrial Radio Access (EUTRA) and Evolved Universal Terrestrial Radio Access Network (E-UTRAN); Overall Description (Release 13)*, document 3GPP TS 136.300, Apr. 2016.

[5] Y.-H. Tsai and T.-H. Sang, "A new timing synchronization and cell search procedure resistant to carrier frequency offsets for 3GPP-LTE downlink," in *Proc. ICCC*, Aug. 2012, pp. 334–338.

[6] A. Golnari, M. Shabany, A. Nezamalhosseini, and G. Gulak, "Design and implementation of time and frequency synchronization in LTE," *IEEE Trans. Very Large Scale Integr. (VLSI) Syst.*, vol. 23, no. 12, pp. 2970–2982, Dec. 2015.

[7] M. R. Sriharsha, S. Dama, and K. Kuchi, "A complete cell search and synchronization in LTE," *EURASIP J. Wireless Commun. Netw.*, vol. 2017, no. 1, pp. 1–14, Dec. 2017, Art. no. 101.

[8] Z. Zhang, J. Liu, and K. Long, "Low-complexity cell search with fast PSS identification in LTE," *IEEE Trans. Veh. Technol.*, vol. 61, no. 4, pp. 1719–1729, May 2012.

[9] A. N. Gaber, L. D. Khalaf, and A. M. Mustafa, "Synchronization and cell search algorithms in 3GPP long term evolution systems (FDD mode)," *WSEAS Transactions on Commun.*, vol. 11, no. 2, pp. 70–81, Feb. 2012.

[10] S.-L. Su, Y.-C. Lin, and Y.-J. Fan, "Joint sector identity and integer part of carrier frequency offset detection by phase-difference in long term evolution cell search process," *IET Commun.*, vol. 7, no. 10, pp. 950–959, Jul. 2013.

[11] M. H. Nassralla, M. M. Mansour, and L. M. A. Jalloul, "A low-complexity detection algorithm for the primary synchronization signal in LTE," *IEEE Trans. Veh. Technol.*, vol. 65, no. 10, pp. 8751–8757, Oct. 2016.

[12] M. Morelli and M. Moretti, "A robust maximum likelihood scheme for PSS detection and integer frequency offset recovery in LTE systems," *IEEE Trans. Wireless Commun.*, vol. 15, no. 2, pp. 1353–1363, Feb. 2016.

[13] R.-L. Chung and J.-W. Huang, "An improved joint detection of integer frequency offset and sector cell index for LTE downlink," in *Proc. IMECS*, Mar. 2013, pp. 1–5.

[14] W.-J. Shin, H. Yang, S. Lee, and Y.-H. You, "Complexity effective integer frequency offset and sector cell detection scheme for LTE downlink system," *Wireless Pers. Commun.*, vol. 75, no. 4, pp. 2371–2381, Apr. 2014.

[15] C.-Y. Chu, I.-W. Lai, Y.-Y. Lan, and T.-D. Chiueh, "Efficient sequential integer CFO and sector identity detection for LTE cell search," *IEEE Commun. Lett.*, vol. 3, no. 4, pp. 389–392, Aug. 2014.

[16] F. J. López-Martínez, E. Martos-Naya, and J. T. Entrambasaguas, "Low complexity cell search scheme for LTE and LTE-advanced mobile technologies," *Comput. Elect. Eng.*, vol. 38, no. 6, pp. 1502–1512, 2012.

[17] J. Myung, J. Kang, Y. Baek, and B. Koo, "Efficient S-SCH detection algorithm for LTE downlink channel," *IEEE Trans. Veh. Technol.*, vol. 63, no. 6, pp. 2969–2973, Jul. 2014.

[18] M. Morelli and M. Moretti, "A maximum likelihood approach for SSS detection in LTE systems," *IEEE Trans. Wireless Commun.*, vol. 16, no. 4, pp. 2423–2433, Apr. 2017.

[19] M. Chiani, D. Dardari, and M. K. Simon, "New exponential bounds and approximations for the computation of error probability in fading channels," *IEEE Trans. Wireless Commun.*, vol. 2, no. 4, pp. 840–845, Jul. 2003.

[20] G. H. Golub and C. F. Van Loan, *Matrix Computations*. Baltimore, MD, USA: The Johns Hopkins Univ. Press, 1996.

[21] *LTE; Evolved Universal Terrestrial Radio Access (E-UTRA); User Equipment (UE) Radio Transmission and Reception (Release 14)*, document 3GPP TS 36.101 V14.3.0, Apr. 2014.

YONG-AN JUNG received the B.S. and M.S. degrees from the Department of Computer Engineering, Sejong University, Seoul, South Korea, in 2011 and 2013, respectively, where he is currently pursuing the Ph.D. degree with the School of Computer Engineering.

His research interests include the areas of wireless/wired communications systems design, spread spectrum transceivers, and system architecture, especially for realizing advanced OFDM communication systems.

MOO-YOUNG KIM received the M.Sc. degree in electrical engineering from Yonsei University, Seoul, South Korea, in 1995, and the Ph.D. degree in electrical engineering from the Royal Institute of Technology (KTH), Stockholm, Sweden, in 2004.

From 1995 to 2000, he was with the Human Computer Interaction Laboratory, Samsung Advanced Institute of Technology. He was also with the Department of Multimedia Technologies, Ericsson Research, and the Spatial Audio Team, Qualcomm Technologies. He is currently with the Department of Electronics and Information Engineering, Sejong University. His research interests include spatial audio signal processing, speech/audio coding, information theory, speech enhancement, and music information retrieval.

HYOUNG-KYU SONG received the B.S., M.S., and Ph.D. degrees in electronic engineering from Yonsei University, Seoul, South Korea, in 1990, 1992, and 1996, respectively.

From 1996 to 2000, he was a Managerial Engineer with the Korea Electronics Technology Institute, South Korea. Since 2000, he has been a Professor with the Department of Information and Communication Engineering, Sejong University, Seoul. His research interests include digital and data communications, and information theory and their applications with an emphasis on mobile communications.

YOUNG-HWAN YOU received the B.S., M.S., and Ph.D. degrees in electronic engineering from Yonsei University, Seoul, South Korea, in 1993, 1995, and 1999, respectively.

From 1999 to 2002, he was a Senior Researcher with the Wireless PAN Technology Project Office, Korea Electronics Technology Institute, South Korea. Since 2002, he has been a Professor with the Department of Computer Engineering, Sejong University, Seoul. His research interests include wireless communications and signal processing with a particular focus on wireless communications systems design, spread spectrum transceivers, and system architecture for realizing advanced digital communication systems, especially for wireless OFDM.